In conclusion, the magnitude of paleotemperature changes in the Mediterranean basin suggests that the temperature drop during glacial phases was higher than in the oceans but could not exceed 11°C and that the correction factor for isotopic changes of the water should be about twice the value used for the oceans, or 2.7 per mil. The combined effects of temperature and of changing isotopic composition of water on the paleotemperature curve give rise to very sharp isotope peaks; but it is still possible to correlate isotopic stages observed in the Mediterranean area with that of the generalized paleotemperature curve for the last 10^5 years.

C. VERGNAUD GRAZZINI
Laboratoire de Géologie Dynamique
Associé au Centre National de la
Recherche Scientifique,
4, Place Jussieu, 75005 Paris, France

References and Notes

1. C. Emiliani, *Quaternaria* **2**, 87 (1955).
2. C. Vergnaud Grazzini and Y. H. Rosenberg, *Rev. Géogr. Phys. Géol. Dyn. Ser. 2* **11** (No. 3), 279 (1969).
3. F. Rotschy, C. Vergnaud Grazzini, G. Bellaiche, H. Chamley, *Palaeogeogr. Palaeoclimatol. Palaeoecol.* **11**, 125 (1972).
4. C. Vergnaud Grazzini and C. Bartolini, *Rev. Géogr. Phys. Géol. Dyn. Ser. 2* **12** (No. 4), 325 (1971).
5. L. Leclaire and C. Vergnaud Grazzini, *C. R. Acad. Sci. Ser. D Sci. Nat.* **275**, 2111 (1972).
6. C. Vergnaud Grazzini, thesis, Université Pierre et Marie, Paris (1973).
7. M. C. Larmande-Renou and J. M. Martin, in *2nd International Symposium on the Chemistry of the Mediterranean* (Colloque International Exploitation Scientifique de la Méditerranée, Rovinj, Yugoslavia, 1972).
8. N. J. Shackleton *Nature (Lond.)* **215**, 15 (1967).
9. J. C. Duplessy, C. Lalou, A. C. Vinot, *Science* **168**, 250 (1970).
10. J. Van Donk, thesis, Columbia University (1970).
11. R. Letolle and C. Vergnaud Grazzini, in "Les méthodes quantitatives d'étude des variations du climat au cours du Pléistocène," *Colloq. Int. Cent. Nat. Rech. Sci.* **219**, 231 (1973).
12. I thank Dr. C. Emiliani for his encouragement and his criticism of this work.

14 February 1975

Phosphine on Jupiter and Implications for the Great Red Spot

Abstract. *A study of the chemistry and photochemistry of the recently discovered phosphine in the atmosphere of Jupiter suggests that the red colorations on this planet result from photochemical production of red phosphorus particles. Chemical-dynamical models of this red phosphorus haze imply that the intensity of the red coloration is a strong function of the strength of vertical turbulent mixing in the atmosphere. If the Jovian Great Red Spot is a region of considerable dynamical activity our model provides a self-consistent explanation for the redness of this region in comparison to the rest of the planet.*

Phosphine (PH_3) has recently been discovered in the atmosphere of Jupiter by Ridgway (*1*), who used a high-resolution Fourier transform interferometer-spectrometer in the wavelength region 8 to 13 μm; it has been reported more tentatively in the atmosphere of Saturn by Gillett and Forrest (*2*), who used a medium-resolution filter-spectrometer in the same wavelength region. These discoveries add an important new dimension to our understanding of the chemistry and photochemistry of these atmospheres.

In some respects the detection of PH_3 on these planets is surprising. Until this discovery, the thermochemical equilibrium models of Jupiter proposed by Lewis (*3*) had been remarkably successful in explaining the observed composition of its visible atmosphere. This model indicated that phosphorus should be present as PH_3 only below the 800°K level in the deep unobservable portion of the atmosphere. Between the 800° and 300°K levels PH_3 is oxidized by H_2O to form P_4O_6, while above the 300°K level P_4O_6 is condensed out as aqueous H_3PO_3. A reasonable explanation for the observation of PH_3 is possible if atmospheric vertical mixing is much faster than the thermochemical reactions converting PH_3 to P_4O_6. Alternatively, if the H_2O volume mixing ratio on Jupiter is as low as 10^{-6}, as recently reported by Treffers *et al.* (*4*), then there may be insufficient oxygen to oxidize PH_3 above the 800°K level.

Some time ago Lewis and Prinn (*5*) proposed that the yellow and brown colorations in the Jovian atmosphere resulted from rapid ultraviolet (UV) dissociation of H_2S and UV irradiation of NH_4HS particles to form elemental sulfur and ammonium and hydrogen polysulfides (*6*). On the other hand, the red coloration of certain regions, in particular the Great Red Spot, has been attributed to colored organic material produced from CH_4 photodissociation (*7*). However, photodissociation rates of PH_3 are about 1000 times greater than those of CH_4, and most of the products of CH_4 dissociation suggested by studies of Jovian aeronomy are colorless (*8*). We argue here that red phosphorus produced from PH_3 dissociation is the dominant red chromophore on Jupiter.

For our study we have utilized a model atmosphere for Jupiter (Fig. 1) which is composed primarily of H_2 and He in their solar abundance ratio of 7 to 1, with a PH_3 volume mixing ratio of 4×10^{-7} (*9*). At pressures less than 800 mbar we have used the temperature profile inferred by Wallace *et al.* (*10*) from the observed infrared emission in methane bands. At pressures exceeding 800 mbar we have adopted an adiabatic lapse rate as implied by the radiative-dynamical equilibrium calculations of Trafton and Stone (*11*).

Phosphine is dissociated by UV of wavelengths less than 2350 Å. Halmann (*12*) and Kley and Welge (*13*) found that its absorption spectrum in the region 1800 to 2350 Å is continuous with a peak at about 1900 Å. The primary photolysis products appear to be PH_2 and H. Becker and Welge (*14*) also detected absorption in the region 1165 to 1470 Å with a peak at 1250 Å, and the primary products here appear to be PH and H_2. We are not concerned with this shorter wavelength absorption here (*15*).

From Tomasko (*16*) and Anderson *et al.* (*17*) we estimate that the column abundance of H_2 above the effective level for penetration of 2068-Å radiation is about 2.7 km amagat (*18*). This level lies at a pressure of 80 mbar, where the temperature is 112°K (Fig. 1). To a sufficient approximation we can take the atmosphere above this level as optically thin to radiation in the region 1850 to 2200 Å while assuming negligible penetration of these wavelengths into the atmosphere below this level (*19*). The photodissociation rate constant, J_1, of PH_3 above the 80-mbar level is then obtained by convolving the incident solar UV radiation intensities at Jupiter (*20*) with the absorption cross sections of PH_3 in the region 1850 to 2200 Å (*12, 13*) and dividing by 4 for a planetary average. This yields $J_1 = 6 \times 10^{-7}$ sec^{-1} above the 80-mbar level, and as discussed above we take $J_1 = 0$ below this level.

The products of photodissociation of PH_3 were first studied by Melville (*21*) and most recently by Norrish and Oldershaw (*22*). These studies suggest the following reaction sequence

$$PH_3 \rightarrow PH_2 + H \quad (1)$$

$$PH_2 + PH_2 \rightarrow PH + PH_3 \quad (2)$$

$$PH + PH \rightarrow P_2 + H_2 \quad (3)$$

$$H + H + M \rightarrow H_2 + M \quad (4)$$

$$P_2 + P_2 + M \rightarrow P_4 + M \quad (5)$$

$$P_4 \rightarrow P_4(s) \quad (6)$$

where M is any background molecule. This sequence appears valid for pressures in the range 0.1 to 1000 mbar and for temperatures ranging from 290° to perhaps as high as 600°K. The products are exclusively red phosphorus [P_4(s)] and H_2. Diphosphine (P_2H_4) is not detectable, and in this respect photodissociation of PH_3 differs significantly from that of NH_3, where hydrazine (N_2H_4) is an important product (*23*).

The quantum efficiency of red phosphorus production, ϕ, in the reaction scheme above is 0.5 if we assume a photochemical steady state for the short-lived species P_2, PH, and PH_2. This is in agreement with experimental results. Other possible reactions of PH_2 such as the three-body reactions

$$PH_2 + H + M \rightarrow PH_3 + M \qquad (7)$$
$$PH_2 + PH_2 + M \rightarrow P_2H_4 + M \qquad (8)$$

apparently do not compete with reaction 2 even for total pressures of 1000 mbar. Norrish and Oldershaw (*22*) argue against the abstraction reaction

$$PH_2 + H \rightarrow PH + H_2$$

competing with reaction 2 even at high temperatures, but add that the abstraction reaction

$$PH_3 + H \rightarrow PH_2 + H_2$$

probably competes with reaction 4 at high temperatures, leading to $\phi \simeq 1$. However, the required high temperatures are not present in the Jovian visible atmosphere.

The reaction sequence 1 through 6 should adequately describe PH_3 photochemistry in the Jovian atmosphere provided that any activation energy associated with reaction 2 is sufficiently small so that it predominates over reactions 7 and 8 even at temperatures as low as 120°K. A reasonable case can be made for this assumption (*24*). Reactions 3 and 5 are exothermic by 57 and 54 kcal/mole, respectively (*25*, *26*), and should both be very rapid. The rate constant for reaction 4 is well known (*27*). Reaction 6 involving nucleation and growth of red phosphorus particles is a proved rapid process with particles of radius $\simeq$ 0.4 μm being detected only a few minutes after PH_3 irradiation (*22*).

The region of stability of red phosphorus particles on Jupiter can be seen in Fig. 1, where we have plotted the vapor pressure of P_4 gas over triclinic red phosphorus (*28*). The vapor pressure scale has been arranged so that if the Jovian temperature profile was identical to the vapor pressure curve the P_4 volume mixing ratio would be 10^{-7} (its maximum possible value in our solar composition atmosphere). Thus in regions where the actual Jovian temperature profile lies to the left of this vapor pressure curve we expect P_4 molecules produced by irreversible PH_3 dissociation to condense as triclinic red phosphorus crystals. These crystals will finally evaporate at or slightly above the point where the two curves in Fig. 1 cross (20 bars, 430°K).

In order to obtain quantitative estimates of red phosphorus particulate densities we have utilized a chemical-dynamical model described by Prinn (*29*) and previously used to simulate the clouds of Venus (*30*). Phosphine is mixed up by turbulent diffusion into the cloud production region above the 80-mbar level where it has a lifetime $(\phi J_1)^{-1} \simeq 38$ days for irreversible conversion to P_4 in red phosphorus. The resultant red phosphorus particles are then transported downward by turbulent diffusion and gravitational sedimentation to a cloud destruction region below the 20-bar level. There they evaporate with a lifetime of 1 hour to yield P_4 gas. The phosphorus cycle is completed below the 800°K level by the thermochemical reaction

$$P_4 + 6H_2 \rightleftarrows 4PH_3$$

which we expect to be fast compared to vertical transport rates. The observability of PH_3 implies that the reaction of P_4 with H_2O to form P_4O_6 between the 430° and 800°K levels is slow relative to vertical mixing.

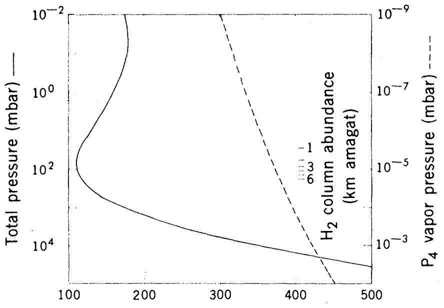

Fig. 1. Total pressure in Jupiter's atmosphere and vapor pressure of P_4 over triclinic red phosphorus crystals as functions of temperature. The column abundance of H_2 above certain levels is also indicated.

By choosing the element P as a tracer we demand that the net flux of P (in PH_3 gas or P_4 particles) through any horizontal surface is zero in a steady-state model. A system of six simultaneous first- and second-order differential equations is obtained from the general equations describing tracer flux and mass continuity. Analytical solutions to this set of equations have been derived for the region below 44 mbar, so the molecular number density of PH_3 and the mass density of red phosphorus can be directly computed. These solutions incorporate a constant atmospheric density scale height of 35 km, and a constant average particulate sedimentation velocity of 1.5 mm/sec. The latter is computed using a particle radius of 1 μm together with the kinematic viscosities of H_2 and He (*25*), and the density of red phosphorus (*25*). At 44 mbar in our model atmosphere the gas mean free path defined by the Chapman-Enskog formula (*31*) equals the particle radius of 1 μm. Above this level the sedimentation velocity increases inversely as the atmospheric density (*32*) and we must solve the appropriate equations by numerical integration with altitude increments of 1 km.

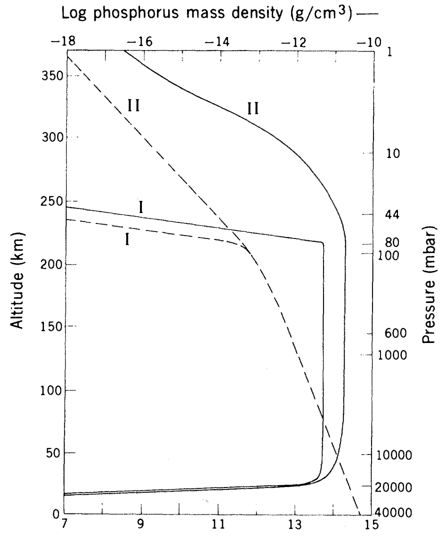

Fig. 2. Mass density of red phosphorus particles and molecular number density of PH_3 gas as functions of altitude and pressure on Jupiter. Run I simulates average planetary conditions and run II simulates the Great Red Spot, which we argue is a region of strong upward mixing.

The results of two runs of our model are illustrated in Fig. 2. Run I is designed to simulate average dynamical conditions on the planet. This run uses vertical eddy diffusion coefficients of 10^4 cm^2/sec in the statically stable region (*33*) above the 80-mbar level, 10^5 cm^2/sec in the partly subadiabatic region between 80 mbar and 20 bars, and 10^6 cm^2/sec in the adiabatic region below the 20-bar level. Run II refers to a region of intense dynamical activity and has a vertical eddy diffusion coefficient of 10^6 cm^2/sec throughout. If the Jovian Great Red Spot is a very long lived storm system (*34*), then the results of run II may be qualitatively applicable to this feature.

Assuming that the particulate extinction cross section is twice the geometrical cross section, the total vertical extinction optical depths of the red phosphorus clouds in runs I and II are 1.1 and 4.4, respectively. Optical depths $\gtrsim 1$ are required to produce an observable coloration. A direct interpretation of these numbers is, however, complicated by the condensation of NH_3 in the visible atmosphere (*3*). Ammonia becomes saturated in our solar composition model at about the 600-mbar level and Weidenschilling and Lewis (*35*) predict ammonia crystal mass densities at this cloud base about 10^4 times greater than the phosphorus mass densities predicted here.

It is doubtful whether phosphorus particle densities exceed those of ammonia crystals except above the tropopause or temperature minimum at 80 mbar. The red phosphorus optical depth above this tropopause is 0.02 (implying essentially no red coloration) in run I and 0.7 (implying significant red coloration) in run II. Thus the strength of the dynamics essentially controls the redness of a particular region: we therefore hypothesize that the coloration of the Great Red Spot is a natural consequence of strong vertical mixing in this locality, as modeled in run II. Phosphorus particles should also be visible in regions where we suspect the ammonia clouds are largely absent, such as the North Equatorial Belt (*5, 6*). The dynamics also clearly affect the PH_3 concentrations above 80 mbar (Fig. 2). In run I vertical transport times are much greater than PH_3 destruction times and PH_3 is severely depleted in the upper atmosphere.

The results presented here for Jupiter can be extrapolated to the other major planets (Saturn, Uranus, and Neptune), where the phosphorus mixing ratios are expected to be $\gtrsim 10^{-7}$. Phosphine may also conceivably be present in the atmosphere of Titan (a satellite of Saturn) and red phosphorus particles may be responsible for its observed red coloration (*36*). Specific models for these other atmospheres together with a consideration of possible cross products of PH_3, NH_3, and CH_4 photodissociation will appear elsewhere (*37*).

RONALD G. PRINN
Department of Meteorology,
Massachusetts Institute of Technology,
Cambridge 02139

JOHN S. LEWIS
Department of Earth and
Planetary Sciences,
Massachusetts Institute of Technology

References and Notes

1. S. T. Ridgway, *Bull. Am. Astron. Soc.* **6**, 376 (1974).
2. F. Gillett and W. Forrest, *Astrophys. J.* **187**, L37 (1974).
3. J. S. Lewis, *Icarus* **10**, 365 and 393 (1969).
4. R. Treffers, H. Larson, U. Fink, T. Gautier, *Bull. Am. Astron. Soc.* **7**, 380 (1975).
5. J. S. Lewis and R. G. Prinn, *Science* **169**, 472 (1970).
6. R. G. Prinn, *Icarus* **13**, 424 (1970).
7. B. N. Khare and C. Sagan, *ibid.* **20**, 311 (1973).
8. D. Strobel, *J. Atmos. Sci.* **30**, 489 (1973).
9. This is approximately the PH_3 mixing ratio in a solar composition atmosphere. Preliminary estimates by Ridgway (*1*) suggest that the observed PH_3 mixing ratio is similar.

→ L. Wallace, M. Prather, M. Belton, *Astrophys. J.* **193**, 481 (1974).

→ L. Trafton and P. Stone, *ibid.* **188**, 649 (1974).

12. M. Halmann, *J. Chem. Soc. (Lond.)* **1963**, 2853 (1963).
13. D. Kley and K. Welge, *Z. Naturforsch. Teil A* **20**, 124 (1965).
14. K. Becker and K. Welge, *ibid.* **19**, 1006 (1964).
15. Wavelengths between 1165 and 1470 Å are absorbed almost totally by CH_4 above the 10-mbar level (*6*). Phosphine concentrations at and above this level are, on the average, negligible (see Fig. 2).
16. M. Tomasko, *Astrophys. J.* **187**, 641 (1974).
17. R. Anderson, J. Pipes, A. Broadfoot, L Wallace, *J. Atmos. Sci.* **26**, 874 (1969).
18. Amagat indicates gas density in units of Loschmidt's number (2.68×10^{19} molecules per cubic centimeter).
19. This lack of further penetration is essentially due to a combination of absorption by PH_3 and NH_3, scattering by H_2 and He, and absorption and scattering by various particulates.
20. E. Schultz and A. Holland, *NASA Contract. Rep. No. CR-11* (1963).

→ H. Melville, *Proc. R. Soc. Lond.* **138**, 374 (1932);

→ *ibid.* **139**, 541 (1933).

→ R. Norrish and G. Oldershaw, *ibid.* **262**, 1 (1961).

23. D. F. Strobel, *J. Atmos. Sci.* **30**, 1205 (1973); S. Gordon, W. Mulac, P. Nangia, *J. Phys. Chem.* **75**, 2087 (1971); M. Hanes and E. Blair, *J. Chem. Phys.* **30**, 672 (1963).
24. Reaction 2 is exothermic by 21 kcal/mole (*13*). The reaction $OH + OH \rightarrow H_2O + O$, which is closely analogous to 2, is exothermic by 17 kcal/mole (*25*) and has an activation energy of 1.1 kcal/mole [D. Baulch, D. Drysdale, D. Horne, A. Lloyd, *Evaluated Kinetic Data for High Temperature Reactions* (Butterworth, London, 1972), vol. 1]. An activation energy $\lesssim$ 1.1 kcal/mole is therefore expected for reaction 2 by analogy.
25. R. C. Weast *et al.*, Eds., *Handbook of Chemistry and Physics* (CRC Press, Cleveland, Ohio, 1973).
26. M. Pannish and J. Arthur, *J. Chem. Thermodyn.* **2**, 299 (1970).
27. D. Ham, D. Trainor, F. Kaufman, *J. Chem. Phys.* **53**, 4395 (1970).
28. J. W. Mellor, Ed., *A Comprehensive Treatise on Inorganic and Theoretical Chemistry*, vol. 8, Suppl. 3, *Phosphorus* (Wiley-Interscience, New York, 1971), pp. 156–167.
29. R. G. Prinn, *J. Atmos. Sci.* **32**, 1237 (1975).
30. ———, *Science* **182**, 1132 (1973).
31. S. Chapman and T. Cowling, *The Mathematical Theory of Non-Uniform Gases* (Cambridge Univ. Press, Cambridge, England, 1952), pp. 74, 218.
32. R. G. Prinn, *J. Atmos. Sci.* **31**, 1691 (1974).
33. Using the vertical temperature gradient above the 80-mbar level (Fig. 1) together with the thermal wind equation [see P. Stone, *J. Atmos. Sci.* **29**, 405 (1972)] and observations of the horizontal temperature gradient by Pioneer 10 and Pioneer 11 we find a Richardson number >> 1, which implies weak vertical mixing. Weak vertical mixing has also been required to explain the altitude distribution of NH_3 (*23*).
34. A. P. Ingersoll, *Science* **182**, 1346 (1973).
35. S. Weidenschilling and J. Lewis, *Icarus* **20**, 465 (1973).
36. T. McCord, T. Johnson, J. Elias, *Astrophys. J.* **165**, 413 (1971).
37. R. G. Prinn and J. S. Lewis, in preparation.

38. We thank J. Richardson for computer assistance and G. Johnson for useful discussions. Supported by NSF grant DES74-14116 and NASA grant NGL-22-009-521. Contribution No. 132 from the MIT Planetary Astronomy Laboratory.

3 March 1975; revised 10 June 1975

Human α-Lactalbumin: Measurement in Serum and in Breast Cancer Organ Cultures by Radioimmunoassay

Abstract. *A sensitive and specific radioimmunoassay for human α-lactalbumin, a major milk protein, is described. Some normal men and women have detectable levels of α-lactalbumin in their blood. High values are found in nursing mothers and many patients with galactorrhea. α-Lactalbumin is found in some breast cancer organ cultures. In addition, α-lactalbumin output was stimulated by ovine prolactin in 2 of the 19 tumors studied.*

The physiology of the human breast has not been extensively studied. Current concepts of mammary endocrinology come mostly from animal studies and cannot always be applied to human problems, particularly those of breast cancer, breast feeding, and galactorrhea. Our interest in human breast physiology is a continuation of mouse breast bioassay studies in which we demonstrated that human prolactin was a molecule which was separate from growth hormone and could be measured in plasma (*1*). Prolactin plays a central role in rat breast growth and development (*2*), normal (*3*) and abnormal lactation (*1, 4*), and appears to influence the growth and spread of some experimental rat breast cancers (*5*). To date, the only well-described mechanism by which prolactin acts is its ability to stimulate milk protein synthesis (*6*). To study the effects of prolactin on the human breast, we have developed a sensitive and specific radioimmunoassay for human α-lactalbumin, a major protein of milk. The α-lactalbumin measurements reported here in human serums and human breast cancer organ cultures appear to be the first of this kind.

A highly purified preparation of human α-lactalbumin (supplied by M. L. Groves) was used in the assay. This preparation, used both for iodination and for standards, migrates as a single band on disc gel electrophoresis (*7*). A potent antiserum to human milk, raised in rabbits, is used. The incubation reaction is carried out for 5 days at 4°C; test samples of 25 μl or less, which represent no more than 1/20 the final incubation volume, were used. All samples were tested in duplicate; the mean difference between duplicates was 6.86 percent. A double antibody system with sheep antiserum to rabbit gamma globulin was used to separate bound from free protein. A representative standard curve and measurements of α-lactalbumin in dilutions of serum from an individual galactorrhea patient with high circulating α-lactalbumin are shown in Fig. 1. The curves are superimposable. This assay is capable of detecting 0.05 ng of α-lactalbumin; the sensitivity for serum samples is 1 ng/ml. No cross-reaction was encountered with high concentrations of human preparations of casein, lysozyme, milk serum albumin, lactoferrin, growth hormone, prolactin, or gamma globulin, or with ovine prolactin, porcine insulin, or fetal calf serum. A high degree of cross-reactivity was observed between the α-lactalbumin of humans and that of other primates (*8, 9*), but not with that of ruminants, supporting previous observations (*10*), or with rodents. As expected, human milk contains large quantities of α-lactalbumin. Samples from two nursing mothers had concentrations of 2.0 and 2.6 mg/ml.

α-Lactalbumin was found in the blood of both lactating and nonlactating men and women (Fig. 2). Of 22 normal males aged 7